DC Performance Testing of MgB_2 Superconducting Straight Wire Samples

Jason W. Hartwig[1], Gerald V. Brown[2], and Benjamin B. Choi[3]
NASA Glenn Research Center, Cleveland, OH, 44135, USA

Frederick W. Vankeuls[4]
Vantage Partners LLC, Brook Park, OH, 44142, USA

Christian Llanes[5]
Embry-Riddle Aeronautical University, Daytona Beach, FL, 32114, USA

Christopher S. Hall[6]
Georgia Institute of Technology, Atlanta, GA, 30332, USA

To enable turboelectric aircraft that utilize fully superconducting motors and generators, testing of high-current, low-AC-loss superconducting wires and coils must be performed. A preliminary investigation was conducted on the critical current capability of a magnesium diboride sample and on the complications that arise from testing the sample with a cryocooler. While a cryocooler provides the benefit of a wide and continuous operating temperature range, cooling a sample by conduction through solid media without a heat-exchange gas is difficult. This paper outlines the hardware and software used to conduct the first DC performance tests on magnesium diboride superconducting samples, along with several check-out tests and mitigation steps needed to produce quality superconducting data using a cryocooler rather than a cryogen.

I. Introduction and Background

This paper presents preliminary superconducting sample data taken as part of a program to enable fully superconducting turboelectric aircraft. The NASA N3-X is a turbo-electric, blended-wing-body concept aircraft using distributed propulsion, which requires superconducting technology development. Several papers have been published on noise and emissions [1], flow simulations [2], propulsion system [3], and the high-power propulsion electrical grid of the NASA N3-X [4]. Felder et al. [3] notes that decoupling the propulsive fans from the power-producing devices will enable performance and design flexibility. As the propulsion power requirement increases, so must the engine size, and it becomes favorable to use electrical transmission networks rather than mechanical transmission. To keep efficiency high, superconducting devices could be used for power transmission, generators, and motors [3]. However, before fully superconducting aircraft can be realized, high-current carrying, low-ac-loss coils for motors and generators must first be developed and tested. AC losses in superconductors arise from several mechanisms, including hysteresis, eddy currents, coupling losses, self-field losses, and other lower order contributions.

A number of superconductors are commercially available that might be considered for the aircraft application, but the need for low ac losses for conductors used in the stators of electric machines narrows the choice. Yttrium barium copper oxide (YBCO) has a critical temperature above the liquid nitrogen (LN_2) boiling point and can sustain high critical currents and magnetic fields. However, YBCO coated tapes have high ac losses due to the wide tape geometry

---

[1] NASA Glenn Research Center, Cleveland, OH, 44135, USA, Fluids and Cryogenics Branch, Associate Fellow
[2] NASA Glenn Research Center, Cleveland, OH, 44135, USA, Rotating Machinery Branch
[3] NASA Glenn Research Center, Cleveland, OH, 44135, USA, Rotating Machinery Branch
[4] HX5, Brook Park, OH, 44142, USA
[5] Embry-Riddle Aeronautical University, Daytona Beach, FL, 32114, USA
[6] Georgia Institute of Technology, Atlanta, GA, 30332, USA

[5]. Attempts have been made to lower ac losses for YBCO by developing striated multifilamentary thin films [6, 7]. The study was successful in showing some reduction in hysteretic losses with minimal degradation of the superconducting properties. Bismuth strontium calcium copper oxide (BSCCO) also has useful current capacity in the 30-60K range but because it too is available commercially only in tape form, it suffers the same drawback as YBCO. On the other hand, magnesium diboride (MgB_2), with a critical temperature of 39K, is of interest because it can carry high current density, can be made into multifilament wires using the powder-in-tube (PIT) process and can be twisted – resulting in lower hysteretic losses. Furthermore, studies have shown that introducing impurities into MgB_2 samples (i.e. doping) changes the superconducting properties [8-14] favorably. Doping increases the critical current density, J_c, and upper critical field, H_{c2}, of MgB_2 with a drawback of yielding a reduced critical temperature, T_c. Overall, it is therefore important to find the optimal doping agent and molar percentage to maximize current carrying capability.

For laboratory evaluation of MgB_2 conductors, liquid hydrogen (LH_2), liquid helium (LHe), gaseous helium (GHe), liquid neon (LNe), gaseous neon (GNe) and cryocoolers can be considered to investigate the superconducting state. LNe is expensive, has the highest boiling point (27.4K) of the cryogens listed and freezes at 24.5K, a range too narrow unless the gaseous state is also used. LHe is expensive but provides the coldest but most narrow operating range. LH_2 is cheaper than LHe, provides better heat transfer properties, but provides only a narrow range of available temperatures. It also presents greater safety issues than many laboratories are willing to accept. GHe may also be a viable choice but presents some difficulties in heat transfer and temperature control. A preferred option is the inherent safety and wide temperature range of the cryocooler to provide cryogenic temperatures, though there are definitely operational complexities involved.

This paper presents MgB_2 superconducting experiments that use a cryocooler as the active heat exchange and discusses pros and cons of using this method. Experiment design, experimental procedure, and uncertainty analysis are discussed. Results are then presented on the cooling system performance, sample performance, and diagnostic test results.

II. Experimental Description

Several MgB_2 samples were tested, all from a single strand of wire manufactured by Hyper Tech Research, Inc. (HTR). Figure 1 is a cross section of the MgB_2 sample. The characteristics of this strand of wire were as follows:

- Barrier: Niobium (Nb)
- Multi sheath: Monel
- Central fill: copper (Cu)
- Powder material: MgB_2 with 2% (molar) of carbon
- Wire diameter: 0.83mm
- Filling factor (volume fraction of superconductor to total volume of wire): 0.123

This strand was manufactured using the continuous tube forming and filling (CTFF) method developed by HTR [15]. The manufacturer first fills the tubes with magnesium and boron powder and then heats the strands, causing the reaction to occur. This is known as the *in-situ* process. Unwanted reactions between the superconducting powder and neighboring material must be prevented, which is the reason why the barrier exists. Three initial samples were used for check-out testing in the cryocooler-based system, one of which was burned out due to a lack of quench detection or protection. The data in this preliminary report is all from the fourth sample.

A cryocooler and the attached experiment were mounted in the multipurpose vacuum vessel shown in Figure 2. The system operating temperature range is 12K-130K. Numerous ports are available for power, instrumentation, fluids, etc. The vessel is operated at high vacuum to minimize gas convection and conduction. A roughing pump was used to achieve 10^{-2} Torr and a turbomolecular pump was used to reach 10^{-5} Torr. Radiation from the room-temperature vessel walls was reduced by aluminum foil sheets placed along the walls of the vessel. These features minimized the parasitic heat leak into the sample and into the cryocooler coldhead and simplified the thermal analysis of the sample and its fixtures.

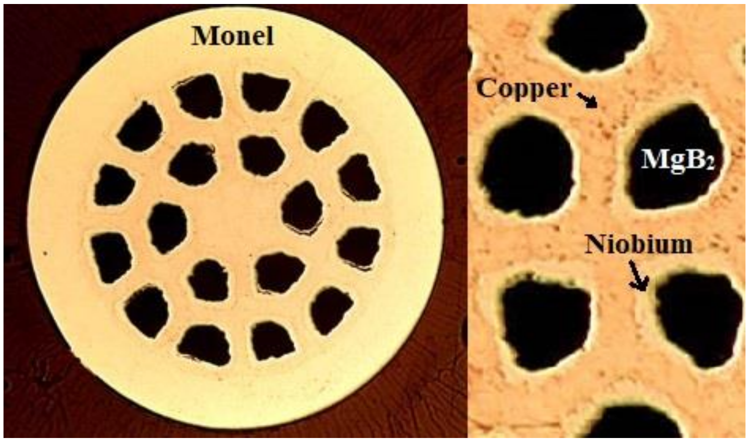

Figure 1. MgB2 cross section from Hyper Tech Research, Inc.

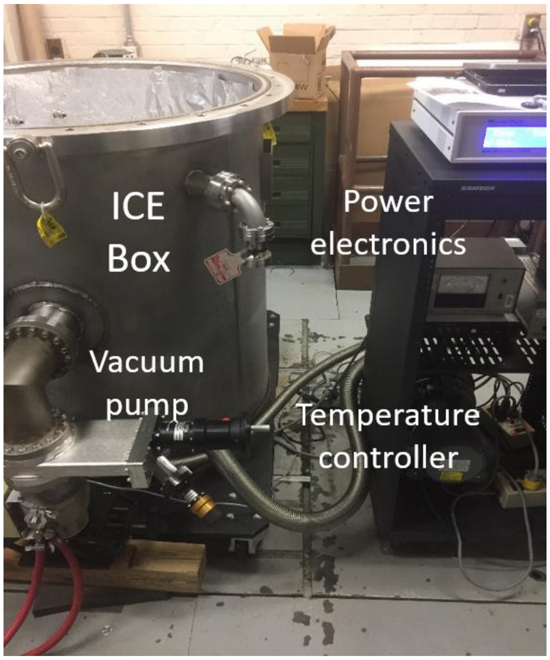

Figure 2. Test Vessel

III. Experimental Design

The cryocooler uses compressed GHe to extract heat from the coldhead inside the vessel. Controlled heat was used to adjust the operating temperature. The electrical system included a sample current power supply, a nanovoltmeter and a temperature controller. The nanovoltmeter sensed voltage across the sample while the temperature controller was used to control and monitor temperature data from seven sensors in the sample space. A LabVIEW program collected data from the various Cernox sensors and the silicon diode temperature sensors.

Figure 3a shows the test setup suspended from the cold head of the cryocooler. There was a long thick copper L-bracket for mounting the MgB_2 short sample and a shorter thick copper L-bracket used as a heat sink for the high-current leads. Eight (four positive and four negative) 16-gauge wires carried current from the room temperature feed-throughs to the heat sink copper plates, which were attached to the shorter L-bracket with a thermally conductive but electrically insulating epoxy with 50-100 micron glass beads. From the heat sink plates to the superconducting sample only two wires per polarity were required because of the higher electrical conductivity of the copper at the low temperature.

Figure 3b shows a diagram of the test setup outlining the location of the various sensors, the MgB_2 test sample, wiring, and the front and back of both L-brackets. The small rectangles labeled A, B, C, D2, D3, and D4 indicate the temperature sensor locations. Sensor D1 (not shown) was placed on the coldhead. Sensors A and C were calibrated silicon diodes, B was a calibrated Cernox, and D1-4 were calibrated silicon diodes. Almost all temperature sensor wires were attached to heat sink copper plates before leaving the vacuum vessel to limit heat leaks into the sensors. The leads for sensors B and C were wrapped around heat sinking spools attached to a copper plate, which in turn attached to the coldhead. Wire pairs were twisted to reduce electromagnetic induction. Temperature sensors had four leads, two wires for current and two voltage across the sensor. This measurement method is known as four-terminal sensing and is used in many measurement devices.

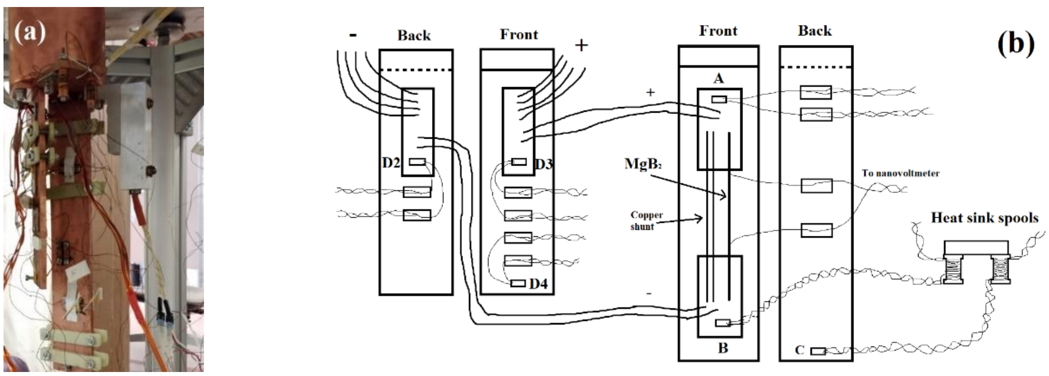

Figure 3. Photo (a) and diagram (b) of test setup. A, B, C, D2-D4 denote temperature sensor locations.

A. Experimental Procedure

The electric field criterion defined by Ekin [16] was used to determine the point at which the superconductor became a "normal" conductor. Ekin mentions that a critical voltage level cannot be chosen because it would change with wire length, therefore a critical electric field value must be chosen. Typically, the critical electric field is chosen as $E_c = 1\ \mu V/cm$. The effective sample length of MgB_2 was 11.5 cm, therefore the defined voltage threshold was 11.5 µV.

Two methods of determining the critical current were tested, and it was found that one method was favored over the other. The first method required fixing the current and then changing the temperature until the nanovoltmeter read 12 µV. The second method, in which temperature is fixed and current is varied, was chosen to conduct DC tests. It was much more difficult to precisely change the temperature of the sample than to change the current, therefore the second method was preferred. This second method produced V-I curves which were used to determine the critical current from Ekin's criteria. All data shown in this paper used the second method.

A heater was used to adjust temperature because the cryocooler has no throttle. The first heater was mounted in an aluminum block and its surface area in contact with the cold head was relatively small, therefore large thermal time constants were observed. An improved heater block made of copper was designed with much larger heat transfer area. Testing showed drastic reduction in response time; results are presented in the next section.

B. Measurement Uncertainty

There are several sources of uncertainty in the data taken. The calibrated silicon diodes have an uncertainty of 31mK at 30K. The calibrated silicon diodes have an uncertainty of 12 mK at 30K. The calibrated Cernox sensors have an uncertainty of 9 mK at 30K. For average temperature data between multiple sensors, such as between sensors A and B, the uncertainty was calculated based on the root-sum-square of the individual uncertainties. The power supply has a front panel display uncertainty of 0.7% + 300 mA of the reading. The nanovoltmeter is accurate to 0.015% of the reading. The vacuum pressure transducer accuracy changes with range; for the pressure ranges of 5×10^{-8} to 10^{-3} Torr, 10^{-3} to 50 Torr, and 50 to 1000 Torr the readings are accurate to 30%, 5%, and 1% respectively. The heater power supply has a front panel display accuracy of 0.1% + 100mV of the reading.

IV. Results and Discussion

A. System Testing

System performance in terms of vessel evacuation and cryocooler cooldown were measured at the outset. Figure 4a shows a typical vacuum vessel pump-down curve using only a roughing pump. Error bars are shown at approximately 5 and 37 minutes. After reaching ~10^{-2} Torr, the cryocooler compressor is turned on, initiating the chilldown shown in Figure 4b. In Figure 4b, MgB_2 Top is sensor A, MgB_2 Bottom is sensor B, and the coldhead sensor is D1. Four other sensors were used but are omitted from the figure for clarity. Error bars are included in this plot at the 5-minute mark. Figure 4b shows that thermally well-connected parts of the system reach roughly 30 K in less than 40 minutes. Continued chilling brings those parts down to ~12K in less than one hour. The sensors attached to points with longer conduction paths, such as the MgB_2 bottom, show longer chill down times.

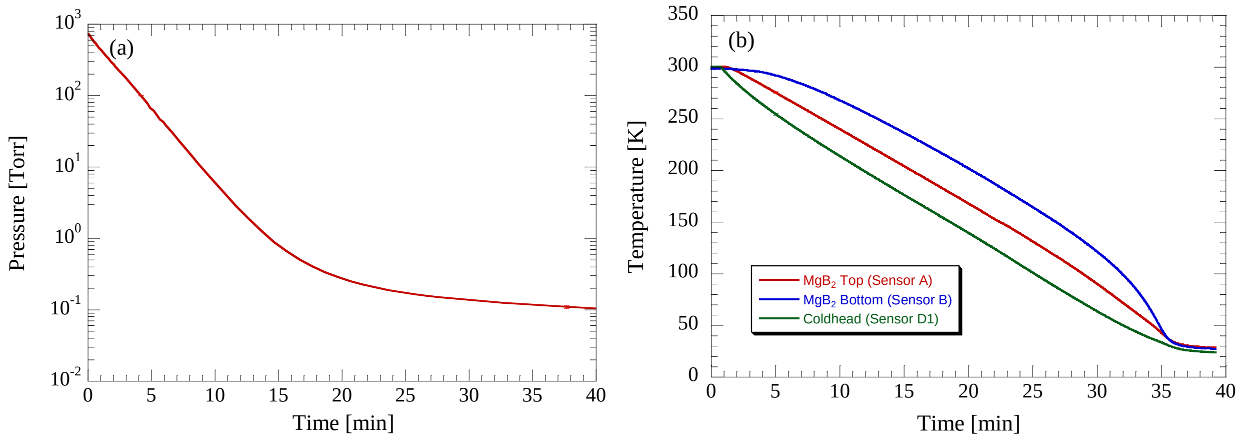

Figure 4. (a) Pump-down curve using only the roughing pump and (b) Chilldown curves for three sensors on test setup.

B. Checkout Testing

Two main check-out tests were conducted to improve the quality of the data. First, accurate temperature measurement and temperature oscillations at steady state were addressed. Secondly the issue of sample quenching and burnout was addressed.

As previously noted, the cryocooler was not “throttle-able”; it runs only at full performance with a cold head temperature that depends on the heat load into the cold head. It delivers a known lift at a given temperature. Heaters were therefore used to regulate the set point temperature. Before passing current through the superconductor, it was desired to have a steady state temperature. Initial test results indicated the existence of temperature fluctuations of up to 3K at a 50K set point irrespective of sensor location as shown in Figure 5a. Oscillations this large are unacceptable due to the highly temperature-sensitive critical current. These oscillations were primarily thought to be inherent to the cryocooler coldhead. Besides the oscillations, it was found that using uncalibrated diodes and Cernox sensors yielded far too much uncertainty in temperature measurements.

Three corrective approaches were implemented to reduce temperature uncertainty: a) using ultra-low uncertainty Cernox sensors, b) correcting/calibrating the remaining sensors, and c) installing a new copper heater block designed with maximum coverage area over the coldhead. The oscillations could only be addressed by closed loop control. The result of a closed-loop proportional-integral-derivative (PID) test is shown in Figure 5b. As shown, there is excellent step response in temperature with voltage. Also, fluctuations across the sample are minimized to < 0.2 K. It was calculated that introducing additional mass in thermal contact with the sample holder and adding some thermal resistance between the heater block and the cold head would reduce oscillations significantly, but this approach has not been implemented.

Second, quench protection and/or detection was addressed. When the MgB_2 sample leaves the superconducting state, rapid heating occurs if high current is still carried through the wire. To prevent damage to the sample in the absence of a quench-detection circuit, a passive shunt in the form of copper wires in parallel to the MgB_2 sample was used such that current would be shared with the shunt when resistance in the MgB_2 sample increased. This presented some uncertainty in the current carried by the MgB_2 sample because the current was only measured externally. The split of current between the superconducting sample and the protective shunt cannot be accurately predicted because of unknown solder joint resistances. However, calculations estimated the approximate error in the current measurement, and it was found that the uncertainty would be negligible if a low resistance solder was used. Previously, indium-tin solder was used for attaching the MgB_2 sample to the copper plates. Calculations indicated that using pure indium solder would reduce the solder joint resistance enough to make the sample current predictable. Pure indium solder has lower resistivity than an indium-tin eutectic alloy but a higher melting temperature. The low resistivity decreased the leakage current uncertainty to the shunt during normal testing.

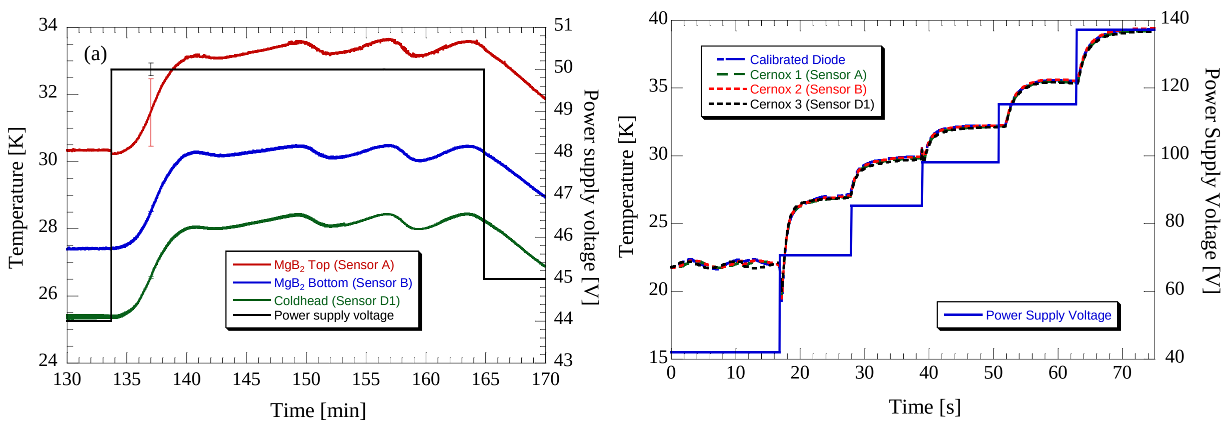

Figure 5. (a) Oscillations of temperature readings from various sensors and (b) Temperature results from new heater block.

However, an external electrical shunt introduced by a controlled system would be a much better tool for the experimental setup because it would eliminate the current uncertainty in the internal parallel conducting path. Another possible approach is controlled shut down. Dubé and Goodrich [17] designed a quench detector circuit using operational amplifiers to detect when the signal voltage from the sample exceeded a reference voltage. The result is a drop in the output voltage, which is sensed by the power supply to shut down the current.

The results of the quench detector circuit are shown in Figure 6 in terms of the circuit input and output voltage. The input to the quench detector is the voltage across the superconductor and the output of the quench detector controls the power supply. During a rapid increase in voltage from the voltage taps on the superconductor (indicating a transition from superconducting to normal behavior), the output voltage of the detection circuit drops from a high state to a low state. This can be sensed to shut down the power supply current. As shown, there is excellent time response, and this drop in output voltage occurs within 250 ms to shut down the power supply.

C. DC Superconducting Testing

Figure 7 shows seven V-I curves for MgB_2 sample #4 at various temperatures near the warmest allowable temperatures for which the sample is still superconducting. Error bars are plotted on the highest voltage measurement for each test, but they are barely discernable. The temperature values shown in the legend of Figure 7 correspond to the average temperature between sensors A and B at the critical current. Figure 7 is an important plot because it depicts the DC transition point from superconducting to the normal state. As shown, as sample temperature decreases, the superconductor critical current increases quite rapidly. Over just a ~2K range from 31 K to 33.2 K, allowable current rises from 2 to 100 A. Although difficult to see in Figure 7, prior to the sharp rise in voltage near the transition point, the voltage across the superconductor is nearly zero for each curve, indicating superconducting behavior. This may be compared with the voltage for a copper wire with the same dimensions which would have a resistance on the order of 40 micro-ohms (assuming a residual resistance ratio of 100, typical for OFHC commercial copper), and at 10 A current, for example, would yield a voltage of 400 microvolts.

From Figure 7, compared to a theoretical critical temperature of 39K for pure MgB_2, the observed critical temperature of the sample at nearly zero current is approximately 33.7K. The disparity may be due to various causes, particularly the result of doping. G Z Li *et al.* [10] reports a critical temperature of 38.2K for non-doped MgB_2, 35.4K for 2% carbon doping, and 33.2K for 3% doping. Doping is used, as mentioned earlier, to increase the critical magnetic field and critical current density.

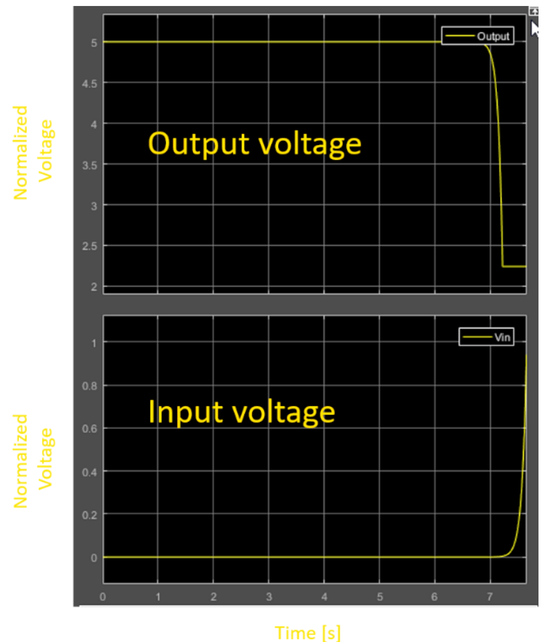

Figure 6. Normalized output and input voltage.

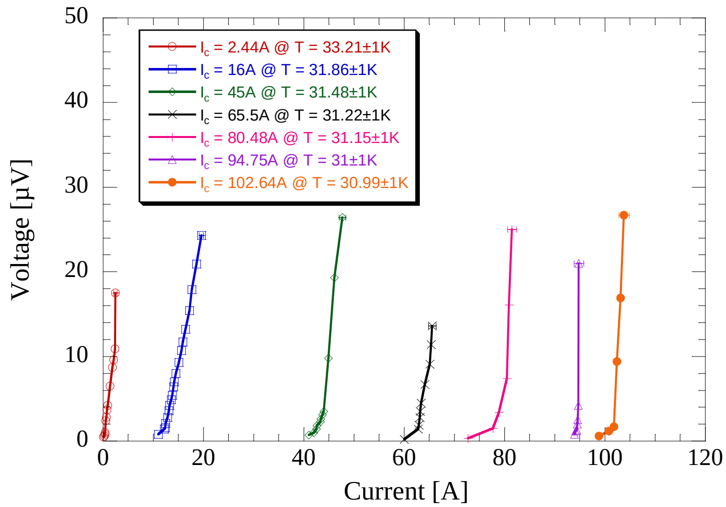

Figure 7. DC test results of MgB2 sample #4. Temperature in this plot is average temperature between sensor A and B.

V. Conclusion

Cryocooler-based cooling for superconductor testing is a more flexible alternative to using conventional liquid or gas cooling, but at the cost of higher operational complexity. This paper presented preliminary MgB_2 short sample data and outlined a few of the difficulties that arise in testing superconductors using cryocooler-based cooling. Issues and mitigation steps are summarized below:

- Temperature sensors – Use properly heat-sinked, calibrated sensors.
- Temperature oscillations – Use closed loop heater control and possibly larger thermal mass near the experiment with some added thermal resistance between the cold head and the experiment.
- Temperature gradient across sample – Shorten thermal conduction path across sample.
- Heating time constants – Use closed-loop control with properly configured proportional-integral-derivative coefficients and ensure that heater and sense resistor are in close proximity.
- Quench and burnout detection – Build a quench detection circuit to monitor sudden increases in superconducting output voltage to shut off power supply current to the sample. At a minimum, use a simple shunt.

Planned future work includes DC testing of multiple other MgB_2 wires, and eventually coils. Afterwards, AC loss tests can commence.

Acknowledgments

This work was funded by the Hybrid Gas Electric Propulsion project under the Aeronautics Research Mission Directorate at NASA Glenn. The authors acknowledge Keith Hunker for his technical comments.

References

1. J. J. Berton, and W. J. Haller, "A Noise and Emissions Assessment of the N3-X Transport", 52nd Aerospace Sciences Meeting, AIAA SciTech Forum, (AIAA 2014-0594)
2. H. Kim, and M. S. Liou, “Flow Simulation of N3-X Hybrid Wing–Body Configuration,” 51st AIAA Aerospace Sciences Meeting, AIAA Paper 2013-0221, Jan. 2013.
3. J. L. Felder, H. D. Kim, and G. V. Brown, "Turboelectric Distributed Propulsion Engine Cycle Analysis for Hybrid-Wing-Body Aircraft", 47th AIAA Aerospace Sciences Meeting, AIAA Paper 2009-1132, Jan. 2009.
4. M. Armstrong, C. Ross, D. Phillips, M. Blackwelder, “Stability, Transient Response, Control, and Safety of a High-Power Electric Grid for Turboelectric Propulsion of Aircraft,” NASA contractor technical report, Rept. NASA/CR-2013-217865, 2013
5. J. P. Murphy, N. N. Gheorghiu, T. Bullard, T. Haugan, M. D. Sumption, M. Majoros, E. W. Collings, "AC loss in YBCO coated conductors at high dB/dt measured using a spinning magnet calorimeter (stator testbed environment)," Cryogenics, 86, 2017, pp. 57-69.
6. C. B. Cobb, P. N. Barnes, T. J. Haugan, J. Tolliver, E. Lee, M. Sumption, E. Collings, C. E. Oberly, "Hysteretic loss reduction in striated YBCO," Physica C: Superconductivity, 382, 2002, pp. 52-56.
7. M.D. Sumpton, “AC Loss of Superconducting Materials for Very High Density Motors and Generators of Hybrid-Electric Aircraft” 2018 Joint Propulsion Conference, Cincinnati, OH, July 9 – 11, 2018.
8. C. B. Eom, M. K. Lee, J. H. Choi, L. J. Belenky, X. Song, L. D. Cooley, M.T. Naus, S. Patnaik, J. Jiang, M. O. Rikel, A. A. Polyanskii, A. Gurevich, X. Y. Cai, S. D. Bu, S. E. Babcock, E. E. Hellstrom, D. C. Larbalestier, N. S. Rogado, K. A. Regan, M. A. Hayward, T. He, J. S. Slusky, K. Inumaru, M. Haas, and R. J. Cava, "High critical current density and enhanced irreversibility field in superconducting MgB2 thin films," Nature, 411, 2001, pp. 558-560.
9. M. Kiuchi, H. Mihara, K. Kimura, T. Haraguchi, E. S. Otabe, T. Matsushita, A. Yamamoto, J. Shimoyama, K. Kishio, "Critical current characteristics in MgB2 bulks," Physica C: Superconductivity and its Applications, 445–448, 2006, pp. 474-477
10. G. Z. Li, Y. Yang, M. A. Susner, M. D. Sumption, E. W. Collings, "Critical Current Densities and n-values of MgB2 Strands over a Wide Range of Temperatures and Fields," Superconductor Science and Technology, 25, 2012.
11. A. Matsumoto, H. Kumakura, H. Kitaguchi, B. J. Senkowicz, M. C. Jewell, E. E. Hellstrom, Y. Zhu, P. M. Voyles, and D. C. Larbalestier, "Evaluation of connectivity, flux pinning, and upper critical field contributions to the critical current density of bulk pure and SiC-alloyed MgB2,"Applied Physics Letters, 89, 2006.
12. Y. Moritomo, and S. Xu, "Effects of transition metal doping in MgB2 superconductor," 2001, Preprint Cond-Mat/0104568
13. B. J. Senkowicz, "Optimizing Critical Current Density through Composition and Microstructure in Mechanically Alloyed Magnesium Diboride" Ph.D. Dissertation, University of Wisconsin-Madison, 2007.
14. M. A. Susner, "Influences of Crystalline Anisotropy, Doping, Porosity, and Connectivity on the Critical Current Densities of Superconducting Magnesium Diboride Bulks, Wires, and Thin Films," Ph.D. Dissertation, The Ohio State University, 2012.
15. D. Doll, M. Tomsic, M. Rindfleisch, C. J. Thong, H. P. J. Yue, T. Wieber, J. Wells, WO Patent No. WO2014109803, (3 Oct. 2013)
16. J. W. Ekin, “Critical-Current Data Analysis,” in Experimental Techniques for Low-Temperature Measurements, New York: Oxford University Press, 2006, pp. 396.